Theory of strongly saturated double-resonance line shapes in arbitrary angular momentum states of molecules

H. W. Galbraith
T-Division, Los Alamos National Laboratory, Los Alamos, New Mexico 87545

Martin Dubs and J. I. Steinfeld
Department of Chemistry and G. R. Harrison Spectroscopy Laboratory, Massachusetts Institute of Technology, Cambridge, Massachusetts 02139
(Received 8 March 1982)

We calculate the steady-state probe absorption line-shape function for a strongly driven, Zeeman-degenerate molecular system. The probe laser is treated to lowest order while the pump laser is dealt with to all orders. We obtain the probe line shape for the cases of parallel and perpendicular linear polarization of the two lasers. As expected, the effects of M degeneracy, as well as differences due to the relative laser polarizations, are most pronounced when Doppler broadening is not important. However, even in the presence of large Doppler broadening we find a narrowing of the population hole by including the Zeeman degeneracy and a further narrowing if perpendicular laser polarizations are used.

I. INTRODUCTION

Optical and infrared double-resonance experiments have proven to be an extremely useful tool for investigating excitation processes in atoms and molecules subjected to intense, resonant fields.[1-3] In particular, the use of tunable infrared diode lasers as probes for molecules such as SF_6,[4,5] or CDF_3,[6] during and after their interaction with CO_2-laser pumping radiation, has begun to shed a good deal of light on the details of the multiple infrared photon excitation process, particularly in the "sparse" regime of discrete vibrational levels. Information can be obtained, from such experiments, concerning both intrinsic atomic and molecular properties, such as transition dipole moments, assignment of vibration-rotation transitions, observation of weak transitions including excited-state absorption, as well as dynamical properties of the system, such as relaxation processes, coherence, and, most recently, the nature of the states involved in multiphoton absorption.[7] Because of its fundamental importance to spectroscopy and dynamics, there has been a considerable amount of work done using double-resonance spectroscopy.[3]

In this paper, we will be concerned primarily with "pump-probe" experiments, in which the pump laser is much stronger than the probe laser, and in general the quantity of interest is the steady-state probe absorption line shape or rate of probe photon absorption versus probe frequency. The two-level double-resonance (2DR) line shape was first given theoretically by Mollow.[8] Mollow's treatment is semiclassical, with fields treated classically and the atomic states quantized. The Bloch equations for the system are reduced to algebraic equations for the probe coherence by treating the probe as a perturbation and equating orders in the probe Rabi frequency. The predicted 2DR line has both absorption and emission (gain) components at saturation. The theoretical line shape has been confirmed experimentally by Wu *et al.*[9] in a Na atomic-beam experiment. The pump and probe lasers were essentially copropagating, with the same polarizations, in that work. Mollow's theory is derived for a nondegenerate two-state system.

In experiments on actual atoms or molecules in high-J states, in which the pump and probe lasers have different polarizations, there will appear dipole-matrix elements coupling the degenerate M_J levels ("Zeeman" degeneracy) with $\Delta M_J = 0, \pm 1$. The M_J-coupling schemes follow from the particular pump-probe relative polarizations, which are the same couplings giving rise to the asymmetries seen in resonance fluorescence. Some of these effects have been treated explicitly by Polder and Schuurmans[10] (for $J=\frac{1}{2}\rightarrow J=\frac{1}{2}$), by Cohen-Tannoudji[11] (for $J=2\rightarrow J=1$ and $J=1\rightarrow J=2$ transitions), and by Cooper *et al.*[12] (for $J=0\rightarrow J=1$, $J=\frac{1}{2}\rightarrow J=\frac{1}{2}$), in the case of resonance fluorescence.

The "three-level"[11,13] double-resonance (3DR) case has been worked out in detail for M-degenerate systems by Hänsch and Toschek[14] and by Feld and

his co-workers.[15] This method has been applied to the measurement of molecular-alignment relaxation rates in ammonia.[16] The explicit M_J dependence for the three-level case has also been dealt with in some detail by Drozdowicz *et al.*[17] Feld has shown[16] that, in the "weak-saturation" approximation, in which the pump laser is treated to second order, the three-level equations can describe a two-level double-resonance experiment. Schwendeman[18] has recently treated the microwave line-shape problem for a two-level system, including the effects of spatial degeneracy under partial saturation, using methods similar to those employed here.

In this paper, we address the question of the effects of laser polarization on M_J-degenerate "two-level"[13] double-resonance experiments under strong pump saturation conditions. We find that the three-level formulas play a new and important role in the line shape at saturation for perpendicular polarizations, but that the bulk of the absorption feature can be described very closely by the Mollow two-level line shape.

II. GENERAL STATEMENT OF THE PROBLEM

We are concerned here with the problem of the excitation of two Zeeman-degenerate levels of angular momenta J_1 and J_2 by a strong pump laser and a weak probe laser. We will solve the equations of motion for this system for the steady-state probe absorption rate (probe line-shape function). The Hamiltonian for our system is divided into a molecular Hamiltonian $\mathscr{H}_M$ and the molecule-field dipole interaction

$$\mathscr{H}=\mathscr{H}_M-\vec{\mu}\cdot(\vec{\mathrm{E}}+\vec{\mathrm{E}}') , \tag{2.1}$$

where $\vec{\mu}$ is the molecular dipole moment operator and $\vec{\mathrm{E}}$ and $\vec{\mathrm{E}}'$ are the pump and probe (classical) electric fields, respectively,

$$\vec{\mathrm{E}}=\frac{\hat{e}\mathscr{E}}{2}(e^{i\omega t}+e^{-i\omega t}) , \tag{2.2}$$

$$\vec{\mathrm{E}}'=\frac{\hat{e}'\mathscr{E}'}{2}(e^{i\nu t}+e^{-i\nu t}) . \tag{2.3}$$

Here $\hat{e},\hat{e}'$ are pump and probe polarization vectors, ω and ν are the frequencies, and $\mathscr{E},\mathscr{E}'$ are field amplitudes. $\mathscr{H}$ is a matrix in the molecular basis set of eigenfunctions of $\mathscr{H}_M$. Quite generally this basis is labeled by the molecular angular momentum and its projection on a laboratory-fixed $\hat{z}$ axis (among other labels)

$$\mathscr{H}_M\,|\,J_\alpha M_\alpha;A\,\rangle=E_\alpha\,|\,J_\alpha M_\alpha;A\,\rangle , \tag{2.4}$$

where $\alpha=1,2$ for ground and excited levels, respectively, and A stands for the set of other labels necessary to specify the molecular eigenstates. (We suppress A in all that follows.) We choose our ground-state energy to be zero and note that both pump and probe lasers are near resonant:

$$\hbar\omega_{12}\equiv E_2-E_1 , \tag{2.5}$$

$$\Delta\omega=\omega-\omega_{12}\ll\omega_{12} , \tag{2.6}$$

and

$$\Delta\nu=\nu-\omega\ll\omega_{12} , \tag{2.7}$$

where ω_{12} is the molecular resonant frequency, $\Delta\omega$ is the pump-laser detuning, and $\Delta\nu$ is the probe-pump detuning.

The matrix elements of the laboratory-fixed components of the molecular-dipole moment μ_σ are, in general, proportional to a Clebsch-Gordan coefficient[19]

$$\langle J_2M_2\,|\,\mu_\sigma\,|\,J_1M_1\,\rangle\propto C(J_1 1J_2;M_1\sigma M_1+\sigma) \tag{2.8}$$

giving an M dependence to the pump and probe Rabi oscillation frequencies. Since $\vec{\mu}$ is a vector operator, we have the J-selection rule

$$\Delta J=-1,0,+1 \tag{2.9}$$

giving the familiar P-, Q-, and R-branch transitions. The M changes for pump and probe fields in (2.1) will depend upon the polarization vectors $\hat{e}$ and $\hat{e}'$ of Eqs. (2.2) and (2.3).

Given the Hamiltonian $\mathscr{H}$ of Eq. (2.1), with matrix elements (2.4) and (2.8), we can form the density-matrix equations of motion

$$\dot{\rho}=\frac{-i}{\hbar}[\mathscr{H},\rho]+\cdots , \tag{2.10}$$

where the ellipsis represents decay terms, with the components $\rho^{J_\alpha J_\beta}_{M_\alpha M_\beta}$ defined as

$$\rho^{J_\alpha J_\beta}_{M_\alpha M_\beta}\equiv|\,J_\alpha M_\alpha\rangle\langle J_\beta M_\beta\,|\,,\quad \alpha,\beta=1,2 . \tag{2.11}$$

The probe absorption rate out of the M_1th sublevel is then just the rate of population flow out of $|\,J_1M_1\,\rangle$ (rate of photon absorption) if the pump laser is off,[8,20]

$$W'_{M_1\to M_2}=-i\frac{\Omega'_{J_1M_1}}{2}(\rho^{J_2J_1}_{M_2M_1}-\rho^{J_1J_2}_{M_1M_2}) , \tag{2.12}$$

where $\Omega'_{J_1M_1}$ is the probe Rabi frequency

$$\Omega'_{J_1M_1}=\frac{1}{\hbar}\langle J_2M_2\,|\,\vec{\mu}\cdot\hat{e}'\,|\,J_1M_1\,\rangle\mathscr{E}' \tag{2.13}$$

and M_2 is related to M_1 by the ΔM selection rules which follow from our choice of polarizations. The

probe line-shape function is then given by

$$W' = \sum_{M_1,M_2} W'_{M_1M_2} . \tag{2.14}$$

Our solution to Eq. (2.10) will be found to all orders in the pump laser Rabi frequency and to lowest order in the probe field strength. Choosing $\hat{e}$, the pump polarization, as our laboratory-fixed $\hat{z}$ axis, we have for the pump laser

$$\Delta M = 0 . \tag{2.15}$$

If the probe laser polarization is parallel to that of the pump, then (2.15) also holds for the probe, but if it is perpendicular we have for the probe

$$\Delta M = \pm 1 . \tag{2.16}$$

The general form of the steady-state probe line-shape function (2.14) is found to be linear and homogeneous in the level populations $\rho^{J_\alpha J_\alpha}_{M_\alpha M_\alpha}$ and proportional to the probe Rabi frequencies. Therefore the lowest-order solution in the probe field strength involves the populations which are found in steady state without the probe. Using the zeroth-order populations we then solve the remaining equations of the set (2.10) for the probe coherences.

III. STEADY-STATE LEVEL POPULATIONS

With the ΔM selection rule (2.15) and ignoring the probe lasers' effect, we can obtain a set of population rate equations. The Bloch equations for the nonzero density-matrix elements are

$$\dot{\rho}^{J_1J_1}_{MM} = \frac{-i\Omega_{J_1M}}{2}(\rho^{J_2J_1}_{MM} - \rho^{J_1J_2}_{MM}) - \sum_{M'} G^{(1)}_{MM'}\rho^{J_1J_1}_{M'M'} - \Gamma_1(\rho^{J_1J_1}_{MM} - \bar{\rho}^{J_1J_1}_{MM}) \tag{3.1}$$

and

$$\dot{\rho}^{J_2J_2}_{MM} = \frac{i\Omega J_1 M}{2}(\rho^{J_2J_1}_{MM} - \rho^{J_1J_2}_{MM}) - \sum_{M'} G^{(2)}_{MM'}\rho^{J_2J_2}_{M'M'} - \Gamma_2(\rho^{J_2J_2}_{MM} - \bar{\rho}^{J_2J_2}_{MM}) \tag{3.2}$$

for the level populations and

$$\dot{\rho}^{J_1J_2}_{MM} = \frac{-i\Omega_{J_1M}}{2}(\rho^{J_2J_2}_{MM} - \rho^{J_1J_1}_{MM}) - z_M\rho^{J_1J_2}_{MM} \tag{3.3}$$

for the pump-induced coherence. Terms such as

$$\sum_{M'} G^{(J_1J_2)}_{MM'}\rho^{J_1J_2}_{M'M'}$$

do not occur, since we assume no coherence decays other than those due to movement of population, i.e., from G diagonal in J_α. In other words, all dephasing is assumed due to population flow, which amounts to a strong-collision assumption.

Equations (3.1) and (3.2) are valid for molecular systems in which collisional relaxation into a bath of rotational states occurs with rates Γ_1 and Γ_2 for the lower and upper vibrational states, respectively. The quantity $\bar{\rho}^{J_\alpha J_\alpha}_{M_\alpha M_\alpha}$ is the equilibrium population of the state $|J_\alpha M_\alpha\rangle$. The coefficients $G^{\alpha}_{MM'}$ give the dipole (orientation) and quadrupole (alignment) relaxation rates in the uncoupled $(\rho^{J_\alpha J_\beta}_{M_\alpha M_\beta})$ basis set[20]

$$G^{(\alpha)}_{MM'} = \sum_k (-1)^{M+M'} \begin{bmatrix} J_\alpha & J_\alpha & k \\ M & -M & 0 \end{bmatrix} \begin{bmatrix} J_\alpha & J_\alpha & k \\ M' & -M' & 0 \end{bmatrix} \times (2k+1) g_k(J_\alpha) \tag{3.4}$$

with $\begin{pmatrix} J_a & J_a & k \\ M & -M & 0 \end{pmatrix}$ and so on being the standard 3-J symbols,[21,22] and $g_k(J_\alpha)$ the kth-rank tensor relaxation rates.

In Eq. (3.3), z is given by

$$z_M = \gamma^{12}_M + i\Delta\omega \tag{3.5}$$

with the pump dephasing rate generally obeying

$$\gamma^{12}_M \geq (\Gamma_1+\Gamma_2)/2 + (G^{(1)}_{MM} + G^{(2)}_{MM})/2 \tag{3.6}$$

with equality in the strong-collision limit. For an infrared transition, spontaneous emission can be neglected, since the radiative lifetime is much longer than any of the other relaxation times in the system.

In steady state, the left-hand sides of Eqs. (3.1)–(3.3) vanish and the pump coherence can be eliminated by solving (3.3) for $\rho^{J_1J_2}_{MM}$ in terms of the populations. We then have

$$\frac{-\Omega^2_{J_1M}\gamma^{12}_M(\rho^{J_1J_1}_{MM} - \rho^{J_2J_2}_{MM})}{2|z_M|^2} - \sum_{M'} G^{(1)}_{MM'}\rho^{J_1J_1}_{M'M'} - \Gamma_1(\rho^{J_1J_1}_{MM} - \bar{\rho}^{J_1J_1}_{MM}) = 0 , \tag{3.7}$$

$$\frac{\Omega^2_{J_1M}\gamma^{12}_M(\rho^{J_1J_1}_{MM} - \rho^{J_2J_2}_{MM})}{2|z_M|^2} - \sum_{M'} G^{(2)}_{MM'}\rho^{J_2J_2}_{M'M'} - \Gamma_2(\rho^{J_2J_2}_{MM} - \bar{\rho}^{J_2J_2}_{MM}) = 0 . \tag{3.8}$$

These equations are linear inhomogeneous equations for the populations and can be solved by standard numerical matrix techniques for arbitrary values of

the parameters $g_k(J)$. If M-changing collisions can be regarded as unimportant compared with Γ_1 or Γ_2 processes, then the major M dependence in the populations comes from the saturating-field Rabi frequencies. If we can ignore the additional M dependence obtained through the $G^{(\alpha)}_{MM'}$, then simple analytic solutions can be found for the populations

$$\rho^{J_1J_1}_{MM} \approx \frac{(\bar{\rho}^{J_1J_1}_{MM}\Gamma_1+\bar{\rho}^{J_2J_2}_{MM}\Gamma_2)\Omega^2_{J_1M}\gamma^{12}+2\bar{\rho}^{J_1J_1}_{MM}|z|^2\Gamma_2\Gamma_1}{\Omega^2_{J_1M}\gamma^{12}(\Gamma_1+\Gamma_2)+2|z|^2\Gamma_1\Gamma_2} \tag{3.9}$$

for the ground-state M levels and

$$\rho^{J_2J_2}_{MM} \approx \frac{(\bar{\rho}^{J_1J_1}_{MM}\Gamma_1+\bar{\rho}^{J_2J_2}_{MM}\Gamma_2)\Omega^2_{J_1M}\gamma^{12}+2\bar{\rho}^{J_2J_2}_{MM}|z|^2\Gamma_1\Gamma_2}{\Omega^2_{J_1M}\gamma^{12}(\Gamma_1+\Gamma_2)+2|z|^2\Gamma_1\Gamma_2} \tag{3.10}$$

for the upper levels.

If we assume instead that the $g_k(J\alpha)$ are not zero, but are much smaller than Γ_1 or Γ_2, we can obtain a perturbation expansion for the populations ${}^{(1)}\rho^{J_\alpha J_\alpha}_{MM}$ by substituting Eqs. (3.9) and (3.10) back into the $\sum_M G^{(\alpha)}_{MM'}\rho^{J_\alpha J_\alpha}_{MM'}$ terms in Eqs. (3.7) and (3.8). This gives

$${}^{(1)}\rho^{J_1J_1}_{MM} = \left[\frac{2J_1+1}{\Gamma_1}\right]{}^{(0)}\rho^{J_1J_1}_{MM}A_M - \left[\frac{2J_1+1}{\Gamma_1}\right]{}^{(0)}\rho^{J_2J_2}_{MM}B_M , \tag{3.11}$$

$${}^{(1)}\rho^{J_2J_2}_{MM} = \left[\frac{2J_1+1}{\Gamma_1}\right]{}^{(0)}\rho^{J_2J_2}_{MM}(A_M-B_M) - \left[\frac{2J_1+1}{\Gamma_2}\right]({}^{(0)}\rho^{J_1J_1}_{MM}-{}^{(0)}\rho^{J_2J_2}_{MM})B_M , \tag{3.12}$$

and

$${}^{(1)}\rho^{J_1J_1}_{J_1J_1} = \frac{1}{2J_1-1} - \sum_{M'}\frac{G^{(1)}_{MM'}}{\Gamma_1}{}^{(0)}\rho^{J_1J_1}_{M'M'} , \tag{3.13}$$

where Eq. (3.13) gives the population of the end states with $M=\pm J_1$. To obtain Eqs. (3.11)–(3.13), we have set $\bar{\rho}^{J_1J_1}_{MM}=1/(2J_1+1)$ and $\bar{\rho}^{J_2J_2}_{M'M'}=0$, corresponding to a filled lower and an empty upper level. The ${}^{(0)}\rho^{J_\alpha J_\alpha}_{MM}$ are from Eqs. (3.9) and (3.10), and

$$A_M = \frac{\Gamma_1}{2J_1+1} - \sum_{M'}G^{(1)}_{MM'}{}^{(0)}\rho^{J_1J_1}_{M'M'} - \frac{\Omega^2_{J_1M}}{4|z|^2}(G^{(1)}_{MM}+G^{(2)}_{MM})\left[\frac{\gamma^2-\Delta\omega^2}{\gamma^2+\Delta\omega^2}\right] , \tag{3.14}$$

$$B_M = \sum_M G^{(2)}_{MM'}{}^{(0)}\rho^{J_2J_2}_{M'M'} - \frac{\Omega^2_{J_1M}(G^{(1)}_{MM}+G^{(2)}_{MM})}{4|z|^2}\left[\frac{\gamma^2-\Delta\omega^2}{\gamma^2+\Delta\omega^2}\right] . \tag{3.15}$$

Also, $\Delta\omega$ is from Eq. (3.5) and $\gamma=(\Gamma_1+\Gamma_2)/2$. These expressions display the behavior of the population to first order in g_k/Γ when $g_k\neq 0$.

We observe from the foregoing that the end-state populations given by (3.13) do suffer a decrease of magnitude

$$(\Gamma_1)^{-1}\textstyle\sum_{M'}G^{(1)}_{MM'}{}^{(0)}\rho^{J_1J_1}_{M'M'} .$$

However, since $\sum_{M'}G^{(1)}_{MM'}=0$, this term is nonzero only because of the M dependence of the zeroth-order level populations, which is due in turn to the M dependence of Ω_{JM}. We have made numerical calculations for $g_k=0.1\Gamma_1$ (a justification for this value is provided in Sec. V). We find negligible differences in the line shapes, as compared with using the analytic expressions (3.9) and (3.10). Indeed, the populations of all but the end states are given accurately by (3.9) and (3.10).

IV. PROBE ABSORPTION LINE-SHAPE FUNCTION

In this section we obtain the probe absorption line shape for the cases of perpendicular and parallel laser polarizations.

A. Perpendicular polarizations

Our pump laser defines the laboratory-fixed $\hat{z}$ axis giving the pump selection rule

$$\Delta M = 0 . \tag{4.1}$$

With probe laser polarization in the $\hat{x}$ direction, we have in polar coordinates

$$\hat{e}' = (\hat{e}_{+1}+\hat{e}_{-1})/\sqrt{2} , \tag{4.2}$$

so that using Eq. (2.8) we have

$$\Delta M = \pm 1 \tag{4.3}$$

for the probe laser. For definiteness we have made our calculations for P transitions $\Delta J=-1$ or

$$J_2 = J_1 - 1 . \tag{4.4}$$

We then have the level-coupling scheme shown in Fig. 1.

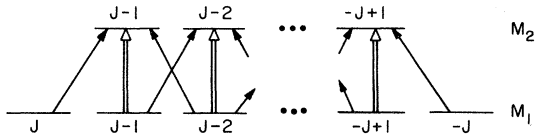

FIG. 1. Coupling scheme for perpendicular polarization in a $P(J)$ transition. For the pump laser, denoted by the double arrows, we have $\Delta M=0$, and for the probe laser (single arrows) we have $\Delta M=\pm 1$.

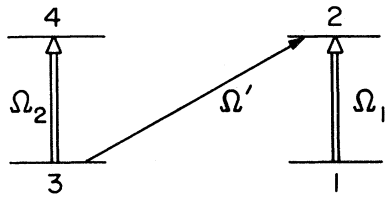

FIG. 2. Laser couplings from Fig. 1 for $M=-J+1,\ldots,J-1$ levels. Ω_1 and Ω_2 are pump Rabi frequencies and Ω' is that for the probe laser.

In the weak-probe approximation, we use the populations of Eqs. (3.9) and (3.10) and keep only those coherences which are of lowest order in the probe, i.e.,

$$\rho^{J_\alpha J_\beta}_{M_\alpha M_\beta}\approx 0 \text{ if } |M_\alpha - M_\beta|>1,\ \alpha,\beta=1,2\ . \tag{4.5}$$

Condition (4.5) leads directly to a decoupling of the various probe coherences from one another. Clearly then the total line-shape function is built up from two generic types of subsystems shown in Figs. 2 and 3. The density-matrix equations for the coherences of Fig. 2 are easily written as

$$\dot\rho_{12}=-z\rho_{12}-\frac{i\Omega_1}{2}(P_2-P_1)+\frac{i\Omega'}{2}\rho_{13}\ , \tag{4.6}$$

$$\dot\rho_{34}=-z\rho_{34}-\frac{i\Omega_2}{2}(P_4-P_3)-\frac{i\Omega'}{2}\rho_{24}\ , \tag{4.7}$$

$$\dot\rho_{23}=(-z^*+i\Delta\nu)\rho_{23}+\frac{i\Omega_2}{2}\rho_{24}-\frac{i\Omega_1}{2}\rho_{13}+\frac{i\Omega'}{2}(P_2-P_3)\ , \tag{4.8}$$

$$\dot\rho_{14}=(-z+i\Delta\nu)\rho_{14}+\frac{i\Omega_2}{2}\rho_{13}-\frac{i\Omega_1}{2}\rho_{24}\ , \tag{4.9}$$

$$\dot\rho_{13}=(i\Delta\nu-\gamma_1)\rho_{13}-\frac{i\Omega_1}{2}\rho_{23}+\frac{i\Omega_2}{2}\rho_{14}+\frac{i\Omega'}{2}\rho_{12}\ , \tag{4.10}$$

$$\rho_{24}=(i\Delta\nu-\gamma_2)\rho_{24}-\frac{i\Omega_1}{2}\rho_{14}+\frac{i\Omega_2}{2}\rho_{23}-\frac{i\Omega'}{2}\rho_{34}\ , \tag{4.11}$$

where z is given by Eq. (3.5) and where for P-branch transitions[19,23]

$$\Omega_{JM}=\frac{\mu\mathscr{E}}{\hbar}\left[\frac{J^2-M^2}{J(2J+1)}\right]^{1/2} \tag{4.12}$$

and

$$\Omega'_{JM}=\frac{\mu\mathscr{E}'}{\hbar}\left[\frac{(J-1\mp M)(J\mp M)}{2J(2J+1)}\right]^{1/2}, \tag{4.13}$$

with $\mu\equiv|\vec\mu|$, for M changes of ± 1. [With the labeling of Fig. 1, $\Omega_1=\Omega_{JM-1}$, $\Omega_2=\Omega_{JM}$, and $\Omega'=\Omega'_{JM}$. P_α are the level populations ($P_1=\rho^{JJ}_{M-1,M-1}$, $P_3=\rho^{JJ}_{MM}$, $P_2=\rho^{J-1,J-1}_{M-1,M-1}$, and $P_4=\rho^{J-1,J-1}_{MM}$)]. Ignoring the $G_{MM'}$ of Eqs. (3.1) and (3.2), we now have for the dephasing rate in the strong-collision limit

$$\gamma_1=\Gamma_1 \tag{4.14a}$$

and

$$\gamma_2=\Gamma_2\ . \tag{4.14b}$$

As in the derivation of the population rate equations, we take for the pump coherences their probe-independent values

$$\rho_{12}\approx\frac{i\Omega_1}{2z}(P_1-P_2) \tag{4.15a}$$

and

$$\rho_{34}\approx\frac{i\Omega_2}{2z}(P_3-P_4)\ . \tag{4.15b}$$

The system of equations (4.8)–(4.11) is then a linear inhomogeneous system for the four probe coherences. The solution for the probe coherence is then easily written in determinantal form:

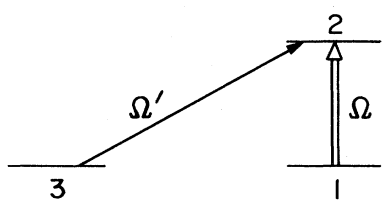

FIG. 3. Laser couplings for $M=\pm J$ in a $P(J)$ transition.

$$\rho_{23}=\frac{\begin{vmatrix} \frac{i\Omega'}{2}(P_2-P_3)/2 & \frac{i\Omega_1}{2}\Big/2 & \frac{i\Omega_2}{2}\Big/2 & 0 \\ \Omega'\Omega_1(P_1-P_2)/4z & (-\gamma_1+i\Delta\nu) & 0 & i\Omega_2/2 \\ \Omega'\Omega_2(P_3-P_4)/4z & 0 & (-\gamma_2+i\Delta\nu) & -i\Omega_1/2 \\ 0 & i\Omega_2/2 & -i\Omega_1/2 & (-z+i\Delta\nu) \end{vmatrix}}{\begin{vmatrix} (-z^*+i\Delta\nu) & -i\Omega_1/2 & i\Omega_2/2 & 0 \\ -i\Omega_2/2 & (-\gamma_1+i\Delta\nu) & 0 & i\Omega_2/2 \\ i\Omega_2/2 & 0 & (-\gamma_2+i\Delta\nu) & -i\Omega_1/2 \\ 0 & i\Omega_2/2 & -i\Omega_1/2 & (-z+i\Delta\nu) \end{vmatrix}} . \tag{4.16}$$

Equation (4.16) is convenient for numerical evaluation. The line shape derived from (2.12) and (4.16) has a structure which is similar to the two-level double-resonance line shape of Mollow.[8] To see this, we set $\gamma_1=\gamma_2=\gamma$ and $\Omega_1=\Omega_2=\Omega$ and obtain (since $P_3=P_1$ and $P_2=P_4$ now)

$$\rho_{23}=i\Omega'(P_2-P_1)\left[\frac{(z-i\Delta\nu)(\gamma-i\Delta\nu)+i\Delta\nu\Omega^2/2z}{(z^*-i\Delta\nu)(z-i\Delta\nu)(\gamma-i\Delta\nu)+\Omega^2(\gamma-i\Delta\nu)}\right] . \tag{4.17}$$

Equation (4.17) is the analog of Eq. (3.11a) of Ref. 8 with the only difference being that we are here treating a scalar relaxation rate which is appropriate for molecules and the Mollow line was derived with atomic relaxation processes in mind. In the calculations below we use only one scalar relaxation rate

$$\Gamma_1=\Gamma_2=\Gamma \tag{4.18}$$

and then Eq. (4.17) is identical to the Mollow function. [Of course, the populations are still given by Eqs. (3.9) and (3.10).]

The recovery of Mollow's result here should not really be surprising if one compares our coupling scheme of Fig. 2 with the dressed-atom picture for the two-level double-resonance problem [see Ref. 9, Fig. 4(b)]. Clearly then we must recover the Mollow result if we have treated the probe laser consistently to lowest order.

By diagonalizing the pump couplings of Fig. 2, we obtain the Stark shifts seen in the probe line shape. The Stark split energies are

$$\lambda_{\pm}^{\alpha}=\frac{-\Delta\omega\pm(\Delta\omega^2+\Omega_\alpha^2)^{1/2}}{2} . \tag{4.19}$$

If the pump laser is near resonant ($|\Delta\omega| \ll \Omega_\alpha$), we have resonant probe absorptions at frequencies

$$S_1\cong\pm(\Omega_1+\Omega_2)/2 , \tag{4.20a}$$

$$S_2=\pm(\Omega_1-\Omega_2)/2 , \tag{4.20b}$$

since levels $|3\rangle$ and $|4\rangle$ can now make transitions to both of the levels $|1\rangle$ and $|2\rangle$ due to the pump mixing of those states. In the Mollow case, we have $\Omega_1=\Omega_2$ and $S_2=0$. As will be seen below, $|S_2|$ cannot be assumed to be a small quantity and our calculations show that the M dependence of the Ω_{J_1M} cannot be ignored. The effect of Eqs. (4.20a) and (4.20b) is to introduce a broadening (or splitting if $|S_2|>\gamma$) to the Mollow line. Clearly, however, it the pump laser is powerful and near resonant the probe absorption of Fig. 2 can be strongly saturated as it is in the Mollow case.

Let us now consider the system of Fig. 3, where levels $|1\rangle$ and $|2\rangle$ have M values $\pm(J-1)$ and level $|3\rangle$ has $M=\pm J$. Bloch equations for the coherences are now obtained from Eqs. (4.6)–(4.11) by setting $\Omega_2=0$ and $\Omega=\Omega_1$:

$$\dot{\rho}_{12}=-\frac{i\Omega}{2}(P_2-P_1)+\frac{i\Omega'}{2}\rho_{13}-z\rho_{12} , \tag{4.21}$$

$$\dot{\rho}_{23}=-\frac{i\Omega'}{2}(P_3-P_2)-\frac{i\Omega}{2}\rho_{13}-\bar{z}\rho_{23} , \tag{4.22}$$

$$\dot{\rho}_{13}=+\frac{i\Omega'}{2}\rho_{12}-\frac{i\Omega}{2}\rho_{23}-z'\rho_{13} , \tag{4.23}$$

where

$$z'=\gamma_{12}-i\Delta\nu \tag{4.24}$$

and

$$\bar{z}=\gamma_{12}-i(\Delta\nu+\Delta\omega) . \tag{4.25}$$

The solution for ρ_{23} is easily found in terms of ρ_{13}:

$$\rho_{23}=-\frac{i\Omega}{2\bar{z}}\rho_{13}+\frac{i\Omega'}{2\bar{z}}(P_2-P_3)\ , \tag{4.26}$$

where

$$\rho_{13}=\frac{\Omega\Omega'}{\Omega^2+4z'\bar{z}}\left[P_2-P_3-\left[\frac{\bar{z}}{z}\right](P_1-P_2)\right]\ . \tag{4.27}$$

Equations (4.26) and (4.27) are convenient for numerical evaluation. By once more diagonalizing the pump-laser coupling we see for a near-resonant pump laser that the probe absorptions are now at Stark frequencies

$$S_3\cong\pm\Omega/2\ , \tag{4.28}$$

i.e., the probe absorptions of Fig. 3 are Stark split by roughly one-half that of those of Fig. 2. The absorption from level 3 leads to a new transition superimposed on the Mollow-like line. It is also clear from Fig. 3 that the pump laser cannot saturate this probe transition, which is characteristic of a three-level double-resonance signal.[14–18] The strength of this absorption feature in the total line shape is inversely proportional to the system angular momentum.

Formally we can write the total probe absorption line shape as a sum over M values of transitions from Figs. 2 and 3

$W'=\sum_M$ (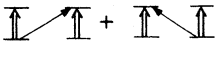) + 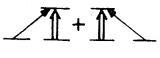 . (4.29)

The first terms on the right-hand side are Mollow-like (except for the M dependence of the pump Rabi frequencies) and characteristic of two-level double-resonance signals,[8,9] while the last two terms are essentially three-level double-resonance signals.[14–17] The probe absorption line shape for the perpendicular-laser polarization case is then characteristic of this superposition.

B. Parallel polarizations

With parallel linear polarizations we have the selection rule $\Delta M=0$ for both pump and probe lasers. This gives the coupling scheme of Fig. 4. The steady-state populations will still be given by Eqs. (3.9) and (3.10) and the total line shape is clearly now a sum over the Mollow function, Eq. (4.17), with the pump and probe Rabi frequencies providing the M dependence. To compare with the single Mollow function, we will replace the sum with the M-averaged value of the Rabi frequencies:

$$\langle\Omega_{JM}^2\rangle=(\mu\mathscr{E}/\hbar)^2/3\ . \tag{4.30}$$

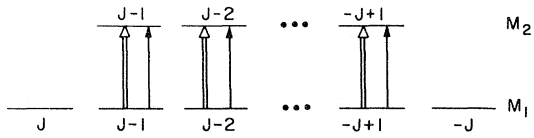

FIG. 4. Coupling scheme for a $P(J)$ transition with parallel laser polarizations.

V. RESULTS AND CONCLUSIONS

In this section we present the results of numerically evaluating the functions (4.16), (4.17), (4.26), and (4.27), and form the M sum Eq. (2.14) to obtain the total probe absorption line-shape function for the cases of parallel and perpendicular polarizations. In some instances, we use the averaged Rabi frequency (4.30) to generate the Mollow line. In our calculations we have fixed our parameters as follows:

$$\frac{\Omega_0}{2\pi}=\frac{\mu\mathscr{E}}{h}=40\ , \tag{5.1}$$

$$\frac{\Omega_0'}{2\pi}=\frac{\mu\mathscr{E}'}{h}=0.02, \tag{5.2}$$

and

$$\frac{\Gamma_1}{2\pi}=\frac{\Gamma_2}{2\pi}=\frac{\gamma}{2\pi}=5 \tag{5.3}$$

with values expressed in units of MHz. Also,

$$\bar{\rho}_{MM}^{J_1J_1}=\frac{1}{2J_1+1}\ , \tag{5.4}$$

$$\bar{\rho}_{MM}^{J_2J_2}=0\ . \tag{5.5}$$

These values roughly correspond to those describing the infrared double-resonance experiments in SF_6.[4,5,24] We further assume that M-changing collisions are unimportant in the problem by setting

$$G_{MM'}^{\alpha}=0,\quad \alpha=1,2\ . \tag{5.6}$$

Several independent experimental and theoretical results lend credence to this assumption. Fluorescence experiments on NaK* in He (Ref. 25) yield total elastic reorientation cross sections $\sigma(\Delta M)\leq 0.3$ Å^2, while total rotational relaxation cross sections $\sigma(\Delta J)$ are 30–100 Å^2. Close-coupled calculations on He + HCl (Ref. 26) give $\sigma(\Delta M)\simeq 1$ Å^2, while $\sigma(\Delta J)\simeq 6-10$ Å^2. Calculations on Ar-N_2 (Ref. 27) give $\sigma(\Delta M)/\sigma(\Delta J)\simeq 0.3$, which is the highest value we have found for this ratio. Optical-optical double-resonance experiments on BaO in a bath of CO_2 give $\sigma(\Delta M)=8.4\pm 2.4$ Å^2 (Ref. 28), while $\sigma(\Delta J)\simeq 50-200$ Å^2 (Ref. 29).

Similar conclusions are drawn from fluorescence experiments on I_2 (Ref. 30) and S_2 (Ref. 31), in which orientation is found to be altered less than rotational state. Corresponding results for polyatomics are less clear, although microwave double-resonance experiments on linear polar molecules such as OCS[32] and FCN[33] suggest that dipolar transitions with $\Delta J = \pm 1$ dominate the collisional transfer; polarized infrared double-resonance experiments[34] on SF_6 and BCl_3 also seem to show a persistance of polarization following energy transfer. Thus, neglecting $G^{\alpha}_{MM'}$ relative to Γ_1 and Γ_2 is most probably a good approximation, particularly in high-J molecules such as we are treating here.

The line-shape function W' is the number of photons absorbed per molecule per second and a typical calculation gives a plot of W' versus the probe-laser frequency for fixed-pump-laser detuning. We have also made calculations in the presence of strong Doppler broadening and we compare our polarization cases in copropagating and counterpropagating configurations for pump lasers on resonance and detuned. Finally our calculations were all made for $J_1 = 10$ or $P(10)$ transitions.

A. Homogeneous broadening

Figure 5 shows the on-resonant probe absorption line for perpendicular (a) and parallel (b) polarizations, while curve (c) gives the Mollow line. The calculations verify the discussion of Sec. IV. The three-level double-resonance components of Fig. 3 appear as the Stark split residual absorptions added to the Mollow-like line in the perpendicular polarization case. By Eqs. (5.1), (4.12), and (4.28), the Stark splitting of those components, in units of MHz, is

$$S_3 = \pm\Omega/2 = 0.37\Omega_0/2 = \pm 7.43 \, . \tag{5.7}$$

The population of the $M = \pm J$ states here is $\sim 10\%$ but the effect on the Mollow gain of curves (b) and (c) is dramatic. This is due to the lack of saturation of those transitions by the pump laser. Comparison of curve (b) with (c) shows the effect of the M dependence of the Ω_{JM} on the line; the Mollow line appears "more coherent."

Figure 6 shows the results with the pump laser now detuned by $+20.0$ MHz. As discussed in Ref. 9, here the Mollow line consists of a Stark shifted absorption feature and a gain line due to a three-photon process. As before, the three-level components show much less Stark shift and lead to the

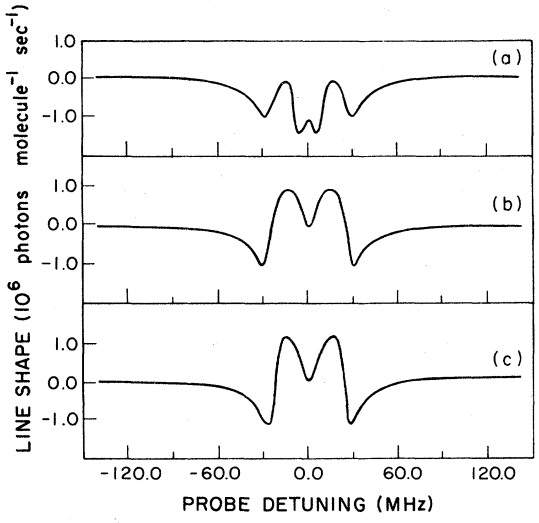

FIG. 5. Probe absorption line-shape function vs probe detuning from the unperturbed molecular resonance frequency. Pump laser is resonant, parameters are given in Eqs. (5.1)–(5.6). Curves (a), (b), and (c) give the perpendicular polarization case, parallel polarization case, and Mollow line, respectively. No Doppler broadening is included here.

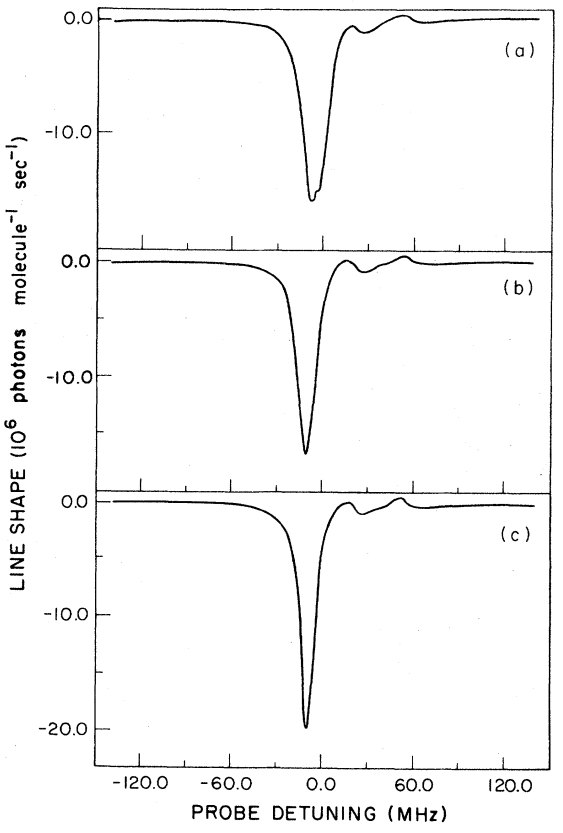

FIG. 6. Same as Fig. 5, with pump laser now detuned by 20 MHz. Curves (a), (b), and (c) as in Fig. 5.

additional absorption component of curve (a). Comparing curves (b) and (c), we again see the slight broadening effects of the M dependence.

B. Doppler broadening

We now consider the line shape of transitions where Doppler broadening is important.[35] In this case the line shape is first evaluated for molecules moving with a velocity $\vec{v}$ and then integrated over a Maxwell-Boltzmann distribution of velocities corresponding to the temperature T. The pump and probe frequencies in a coordinate system attached to the molecule are

$$\omega' = \omega - s \ , \tag{5.8}$$

$$\nu' = \nu - \epsilon s \ , \tag{5.9}$$

$$s = \vec{k}\cdot\vec{v}, \quad |\vec{k}| \cong \omega_{12}/c \ , \tag{5.10}$$

where $\vec{k}$ denotes the propagation vector of the pump beam, $\epsilon = +1$ for copropagating beams and $\epsilon = -1$ for counterpropagating beams. The velocity distribution as a function of s is given by

$$P(s) = \frac{1}{s_0\sqrt{\pi}} \exp(-s^2/s_0^2) \ , \tag{5.11}$$

$$s_0 = \frac{\omega_{12}}{c}\sqrt{2kT/m} \tag{5.12}$$

[where k= Boltzmann constant, m =mass of molecule, and the full Doppler width at half maximum (FWHM) $= 2\sqrt{\ln 2}\, s_0$], which leads to the double-resonance line shape

$$W(\omega,\nu) = \int_{-\infty}^{\infty} ds\, P(s) W(\omega - s, \nu - \epsilon s) \ . \tag{5.13}$$

A key quantity in our calculation is $\Delta\nu$, the probe-pump detuning, which undergoes no shift in the copropagating case and a shift of $2s$ in the counterpropagating case. This leads to a much greater apparent coherence in copropagating signals.

Figure 7 gives the on-resonant copropagating calculation corresponding to Fig. 5, with a Doppler half-width of 40 MHz. Now the M-dependent broadening is almost totally masked by the Doppler broadening, and the parallel polarization line and Mollow line are virtually alike. However, the three-level components remaining unsaturated give much less hole burning in the perpendicular polarization case. Not only is the saturation much less, but the hole shape is distorted or "filled in" because of the smaller Stark shifts of the strongly absorbing three-level components.

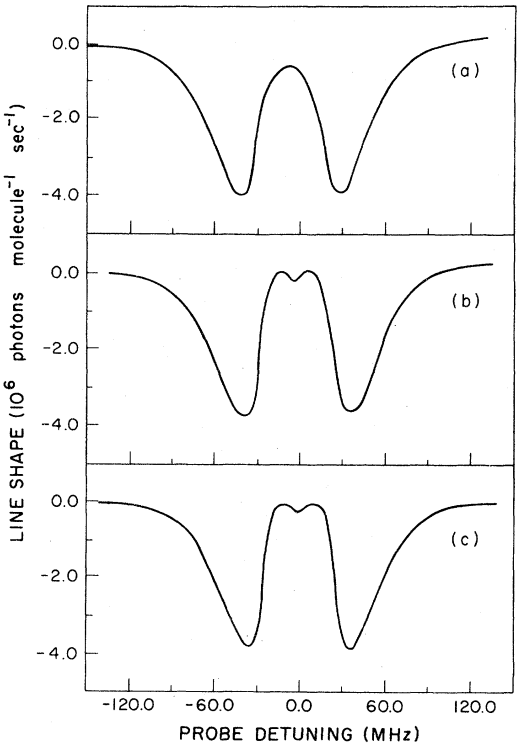

FIG. 7. Absorption lines with pump laser resonant in copropagating geometry, including Doppler broadening. Doppler half-width is 40 MHz. Curves (a), (b), and (c) as in Fig. 5.

Figure 8 shows a comparison of parallel and perpendicular polarizations in counterpropagating geometry. The hole burning is greatly reduced from the copropagating case, but the degree of saturation

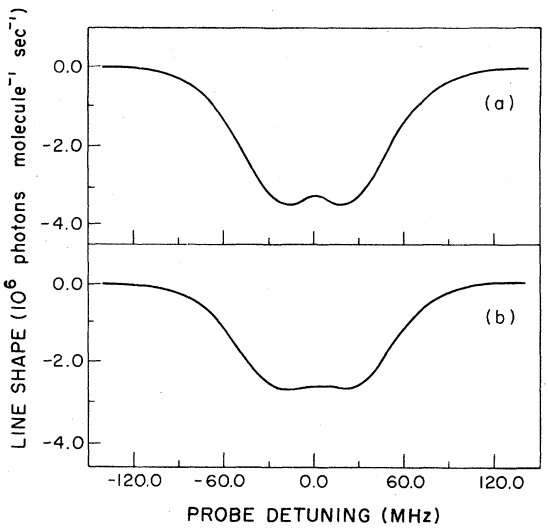

FIG. 8. Same as Fig. 7 but omitting curve (c) and computed in counter propagating geometry.

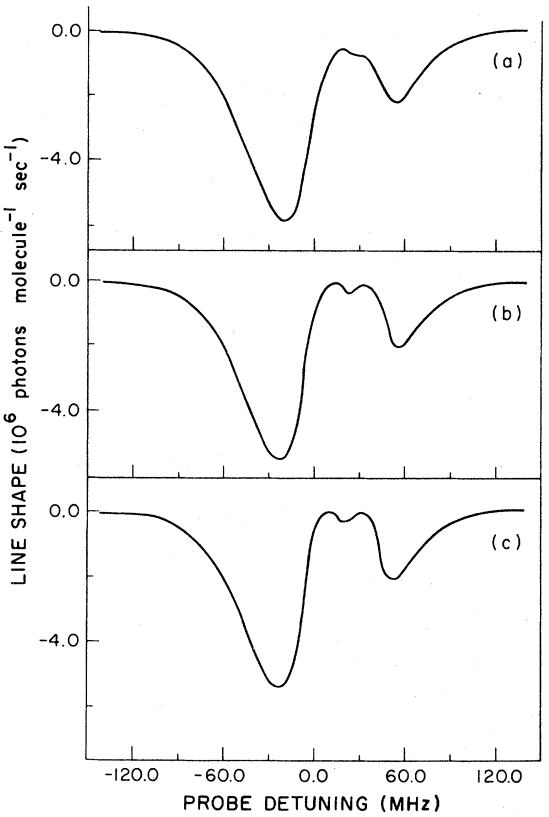

FIG. 9. Same as Fig. 7 with pump laser detuned by 20 MHz.

in case (a) is still much less than in case (b), the discrepancy in peak absorptions being ~20% of the peak value.

Figures 9 and 10 are the off-resonant pump calculations for copropagating and counterpropagating geometries, respectively. In Fig. 9 we see that the polarization effect is less with the pump laser off resonance than in the resonant case of Fig. 7. Again with strong Doppler broadening the Mollow line represents the parallel polarization case quite well. Figure 10 gives a comparison of the detuned pump case in counterpropagation and shows that the polarization saturation discrepancy has dropped to 15% of the peak absorption. Here the population hole is barely visible and is on the negative detuning side of the absorption line.

In summary, we have found that there are substantial qualitative as well as quantitative differences in the probe absorption line shape seen in parallel versus perpendicular relative polarization cases. These differences are fundamentally due to the three-level components of the signal absorption line and are most strongly manifest on-resonance and for small values of the molecular angular momentum. We have also seen that even with substantial Doppler broadening and at fairly substantial J values, the effects are still easily seen in the hole shape and depth in copropagating experiments and in the degree of saturation in counterpropagating geometries.

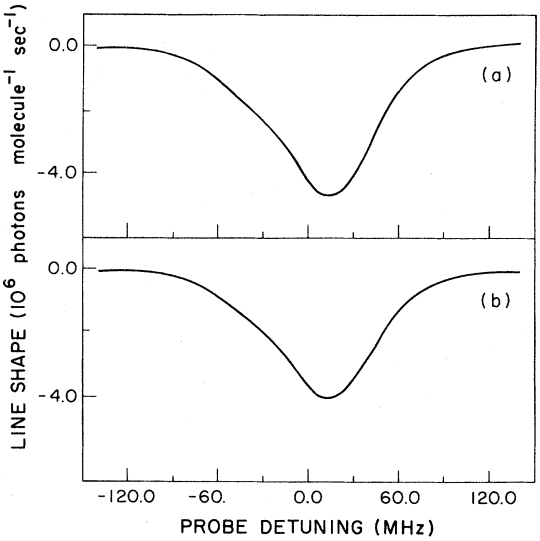

FIG. 10. Same as Fig. 8 with pump laser detuned by 20 MHz.

ACKNOWLEDGMENTS

This work was supported by the National Science Foundation Grant No. CHE80-10803. We would like to thank Jay Ackerhalt, Chris Patterson, Russell Pack, and Professor Michael Feld for helpful discussions. A part of this work was performed while H. W. Galbraith was visiting scientist at the M.I.T. Regional Laser Center, which is a National Science Foundation Regional Instrumentation Facility.

[1]K. Shimoda and T. Shimizu, Prog. Quantum Electron. 2, 45 (1972).

[2]K. Shimoda, in *Topics in Applied Physics Vol. 2, Laser Spectroscopy of Atoms and Molecules,* edited by H. Walther (Springer, Berlin, 1976), pp. 197—252.

[3]P. L. Houston and J. I. Steinfeld, in *Laser and Coherence Methods in Spectroscopy,* edited by J. I. Steinfeld, (Plenum, New York, 1977), pp. 1—123.

[4]C. C. Jensen, T. G. Anderson, C. Reiser, and J. I. Steinfeld, J. Chem. Phys. 71, 3648 (1979).
[5]P. F. Moulton, D. M. Larsen, J. N. Walpole, and A. Mooradian, Opt. Lett. 1, 51 (1977).
[6]M. Dubs, K. Harradine, and Zhu Qingshi (unpublished).
[7]C. W. Patterson, R. S. McDowell, P. F. Moulton, and A. Mooradian, Opt. Lett. 6, 93 (1981).
[8]B. R. Mollow, Phys. Rev. A 5, 2217 (1972).
[9]F. Y. Wu, S. Ezekiel, and B. R. Mollow, Phys. Rev. Lett. 38, 1077 (1977).
[10]D. Polder and M. F. H. Schuurmans, Phys. Rev. A 14, 1468 (1976).
[11]C. Cohen-Tannoudji and S. Reynard, J. Phys. Lett. 38, L173 (1977).
[12]J. Cooper, R. J. Ballagh, and K. Burnett, Phys. Rev. A 22, 535 (1980).
[13]By "two-level" in this context, we mean here two J states, having $J=J''$ for the ground state and $J=J'$ for the excited state, each of which is actually a manifold of M_J states, $2J+1$ in number. "Three-level" means three such J states, with the two radiative transitions having one of the states in common.
[14]Th. Hänsch and P. Toschek, Z. Phys. 236, 213 (1970).
[15]M. S. Feld, M. M. Burns, T. U. Kuhl, and P. G. Pappas, Opt. Lett. 5, 79 (1980); D. E. Murnick, M. S. Feld, M. M. Burns, T. U. Kuhl, and P. G. Pappas, in *Laser Spectroscopy IV,* edited by H. Walther and K. W. Rothe (Springer, Berlin, 1979), p. 195; N. Skribanowitz, M. J. Kelly, and M. S. Feld, Phys. Rev. A 6, 2302 (1972).
[16]J. R. R. Leite, M. Ducloy, A. Sanchez, D. Seligson, and M. S. Feld, Phys. Rev. Lett. 39, 1465 (1977); 39, 1469 (1977).
[17]Z. Drozdowicz, R. J. Temkin, and B. Lax, IEEE J. Quantum Electron. QE-15, 170 (1979).
[18]R. H. Schwendeman, J. Chem. Phys. 73, 4838 (1980).
[19]M. E. Rose, *Elementary Theory of Angular Momentum* (Wiley, New York, 1957), p. 32ff.
[20]L. Allen and J. H. Eberly, *Optical Resonance and Two-level Atoms* (Wiley-Interscience, New York, 1975).
[21]A. Omont, Prog. Quantum Electron. 5, 69 (1977).
[22]D. M. Brink and G. R. Satchler, *Angular Momentum,* 2nd ed., (Clarendon, Oxford, 1968), p. 136.
[23]G. Herzberg, *Molecular Spectra and Molecular Structure. II. Infrared and Raman Spectra of Polyatomic Molecules* (Van Nostrand, Princeton, 1945), p. 421 ff.
[24]C. Reiser, J. I. Steinfeld, and H. W. Galbraith, J. Chem. Phys. 74, 2189 (1981); M. Dubs, D. Harradine, E. Schweitzer, J. I. Steinfeld, and C. Patterson, J. Chem. Phys. (in press).
[25]J. McCormack, A. J. McCaffery, and M. P. Rowe, Chem. Phys. 48, 121 (1980).
[26]L. Monchick, J. Chem. Phys. 67, 4626 (1977); L. Monchick and D. J. Kouri, *ibid.* 69, 3262 (1978).
[27]M. H. Alexander, Chem. Phys. 27, 229 (1978); R. T. Pack, J. Chem. Phys. 62, 3143 (1975).
[28]S. J. Silvers, R. A. Gottscho, and R. W. Field, J. Chem. Phys. 74, 6000 (1981).
[29]R. A. Gottscho, R. W. Field, R. Bacis, and S. J. Silvers, J. Chem. Phys. 73, 599 (1980).
[30]R. B. Kurzel and J. I. Steinfeld, J. Chem. Phys. 56, 5180 (1972).
[31]T. A. Caughey and P. R. Crosley, Chem. Phys. 20, 467 (1977).
[32]R. M. Lees, J. Mol. Spectrosc. 69, 225 (1978).
[33]H. Jones, Appl. Phys. Lett. 31, 268 (1977).
[34]D. S. Frankel and J. I. Steinfeld, J. Chem. Phys. 62, 3358 (1975).
[35]In this connection, we note that velocity-changing collisions have been ignored in this treatment, but that under strong saturation conditions, in which the pumped-velocity group is a sizable function of the Doppler profile, the effect of velocity-changing collisions should be minimal.